OBSERVATION OF HIGHER HARMONIC CORONAL LOOP OSCILLATIONS

I. De Moortel[1] and C.S. Brady[1]

Draft version April 12, 2007

ABSTRACT

A sequence of TRACE 171 Å observations taken on 13 May 2001 shows evidence of flare-induced, transverse coronal loop oscillations (Schrijver et al 2002; Aschwanden et al 2002). We revisit this particular data set and present evidence of the presence of spatially resolved higher harmonics in the transverse loop displacements. The oscillations are identified as the second harmonic, fast MHD, kink waves (periods of 577 - 672 sec), with higher harmonics (250 - 346 sec) also present. The apparent absence of the fundamental mode and the fact that it is the second harmonic (P_2) which dominates the oscillatory behaviour of this particular loop may shed more light on either the excitation and/or the damping mechanism(s) of flare-induced, transverse loop oscillations.

Subject headings: Sun:Oscillations, Sun:Corona, MHD, Waves

1. INTRODUCTION

The advent of space-based satellites has provided us with a wealth of high quality observational data, with unprecedented cadence and spatial resolution. A multitude of wave-like perturbations and oscillations have now been identified in the solar atmosphere, allowing coronal seismology to develop from a theoretical possibility to an active and viable area of research (see e.g. reviews by Nakariakov & Verwichte (2005) and De Moortel (2005)). The study in this manuscript focuses on transverse oscillations of coronal loops, induced by a nearby explosive event. Such loop oscillations have been investigated previously by several authors (Aschwanden et al 1999; Nakariakov et al 1999; Schrijver et al 2002; Aschwanden et al 2002; Verwichte et al 2004) and have been identified as impulsively generated, standing, fast magnetoacoustic kink modes. Based on a sample of 26 examples, Schrijver et al (2002) and Aschwanden et al (2002) find periods of the order of $P = 5.4 \pm 2.3$ min, with relatively short damping times of $\tau_d = 9.7 \pm 6.4$ min. Following the method outlined by Roberts et al (1984), Nakariakov & Ofman (2001) used a combination of basic MHD wave properties and the observed parameters to deduce an estimate for the magnetic field strength of the oscillating coronal loops. Although the associated uncertainties are relatively large, this study clearly demonstrates the potential of coronal seismology.

The potential seismological value of higher harmonics was demonstrated by McEwan et al (2006), who investigated how the ratio of the fundamental period to twice the period of the second harmonic, $P_1/2P_2$, can be used as a diagnostic tool. These authors show that stratification along a coronal loop causes this ratio to depart from unity and hence, an observed shift from unity would yield information on the internal, longitudinal, structuring of a coronal loop. Unfortunately, observations of higher harmonics in coronal loops are very scarce and so far, only two examples have been reported (Verwichte et al 2004). However, in both cases, the higher harmonics were not actually spatially resolved in the observations but their existence was inferred from the presence of multiple periods in a wavelet transform.

To our knowledge, this paper analyses, for the first time, spatially resolved observations of higher harmonics in flare-induced, transverse coronal loop oscillations. The observations and processing of the data are described in Sect. 2. Sect. 3 contains the method and the results of the data analysis. A subsequent discussion and conclusions are presented in Sect. 4.

2. OBSERVATIONS AND DATA PROCESSING

The sequence of 176 TRACE 171 Å 768 × 768 images (with a pixel size of 0.5″) of AR9455 were taken on 13 May 2001 (0252-0430 UT). The data have been subject to standard processing using the IDL SSW routine trace_prep; cosmic ray spikes have been removed and the data were derippled and destreaked. Variations in pointing during the observational sequence and solar rotation were also (manually) corrected for.

The oscillatory behaviour of these coronal loops has been investigated already by Schrijver et al (2002) and Aschwanden et al (2002). These authors give a basic period of 428 sec, present for 664 sec from 0318 UT onwards. Although they mention that a node seems to be present midway along the loop (Schrijver et al (2002) - Appendix Case 15), they do not investigate the apparent presence of higher harmonics and the subsequent analysis by Aschwanden et al (2002) only takes into account the top half of the loop (i.e. they consider the apparent node to be a footpoint). For a high quality movie of the data sequence, we refer the reader to the original movie of Schrijver et al (2002) (Case 15) at http://vestige.lmsal.com/TRACE/POD/TRACEoscillations.html.

3. DATA ANALYSIS

An M3.6 class flare occurs at 02.58 UT in AR9455, inducing oscillations in the nearby loop system, which is shown in Fig. 1. In the images immediately following the flare, much of the loop is obscured in the noisy data but the brighter section near the loop apex remains visible. To obtain loop displacements perpendicular to the loop axis, we chose two loop footpoints, at (-107,-249) and (-69,-441), marked by stars in Fig. 1. We then chose four different cross sections, perpendicular to the line

[1] School of Mathematics and Statistics, University of St Andrews, North Haugh, St Andrews, Fife KY16 9SS, UK

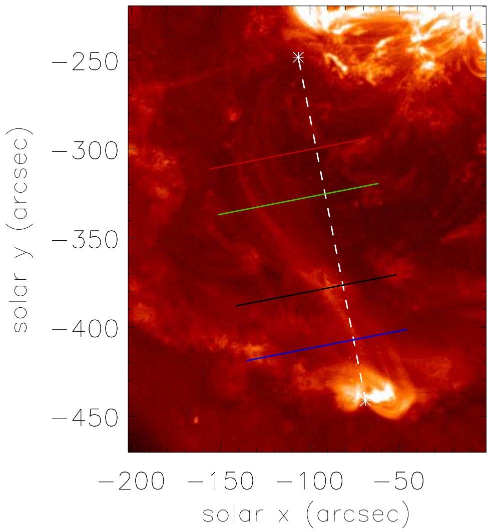

Fig. 1.— TRACE 171 Å image of the oscillation loop at 03.41 UT. Overplotted are the cross-sections ‘upper1’ (red), ‘upper2’ (green), ‘central’ (black) and ‘lower’ (blue).

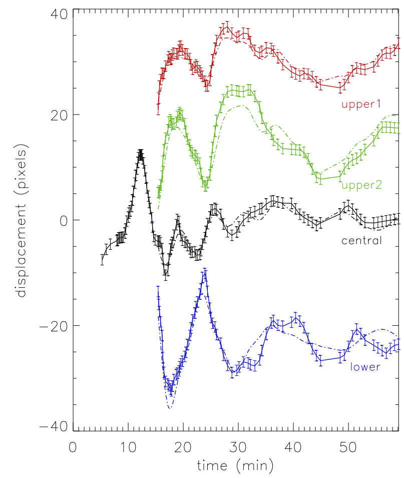

Fig. 2.— Loop displacement at the four cuts across the loop, as a function of time where dot-dashed lines show the corresponding fits. Note that the displacements have been shifted by arbitrary constants.

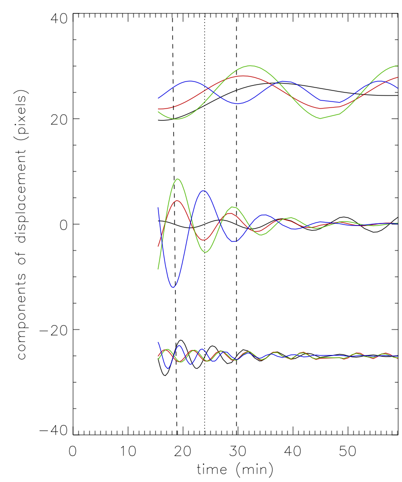

Fig. 3.— Oscillatory components of the respective fits. The vertical dashed and dotted lines correspond to maxima and a minimum of the measured loop displacements. Note that the lines have been shifted by arbitrary constants.

connecting the two footpoints (dashed line). These cross sections, along which we will measure the loop displacement are marked by coloured lines in Fig. 1 and we will refer to the respective locations as ‘upper 1’ (red), ‘upper 2’ (green), ‘central’ (black) and ‘lower’ (blue). Looking at an animated sequence of this dataset, the ‘central’ position looks close to the most likely position of the loop apex. For each timestep, the position of the loop is determined interactively by positioning the cursor over the loop and the perpendicular distance of this position to the loop axis (dashed line in Fig. 1) is calculated. This process is repeated for each of the four positions. Subsequently, a linear fit (possibly corresponding to a small, gradual motion of the entire loop - see Table 1 for the coefficients of the linear fit) is subtracted from each of the oscillations and the resulting loop displacements are shown in Fig. 2. As pointed out above, the fainter parts of the loop are hard to identify immediately after the flare, which is why the curves at ‘upper1’, ‘upper2’ and ‘lower’ start at a slightly later time (03.08-03.51 UT) than ‘central’ (02.57-03.51 UT).

We will investigate the nature of the loop oscillations further in Sect. 4 but first, we will verify the accuracy of the method of determining the displacements by eye. Naturally, this method of measuring loop positions is to some extent subjective. However, in this particular case, the closeness of many faint loop strands makes a user-interactive method more reliable than ‘automated’ methods such as fitting a Gaussian curve to the observed intensity to determine the loop position. We have used two different ways to obtain additional confirmation of the measured displacements. Firstly, in Fig. 4, the intensity, along part of the respective cross sections, is plotted as a function of time and overplotted are the corresponding loop displacements. Note that these intensities were obtained by summing over 6 pixels in the direction perpendicular to the cross sections. From Fig. 4, it is clear that the displacements determined by our user-interactive method agree very well with the actual observed intensities.

As an alternative confirmation of our loop positions, we used a fifth order polynomial interpolation, using the four loop displacements and the two (fixed) footpoints as interpolating points. This ‘fitted’ loop was then overplotted on the observed intensities (see e.g. Fig. 5) and an animated sequence confirmed that the polynomial fit is a good match for the oscillating loop throughout the data set. However, to account for the subjective nature of the determination of the loop displacements, we will associate a one-pixel error with the loop positions, represented by the error bars shown in Fig. 2.

4. DISCUSSION & CONCLUSIONS

Let us now return to Fig. 2 to look more closely at the oscillatory nature of the displacements. The central (apex) oscillation initially shows a relatively large peak,

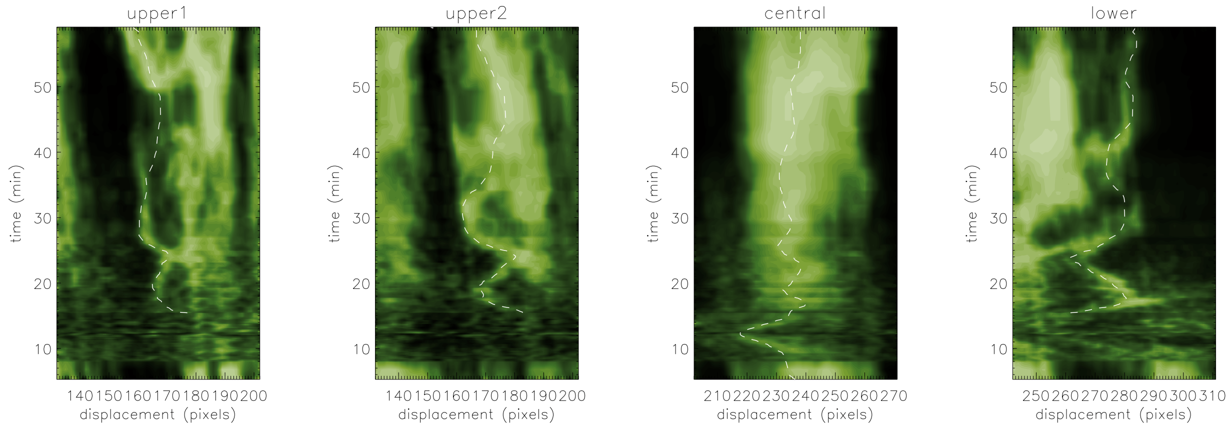

FIG. 4.— Loop displacement (dashed lines) at the four cuts across the loop. The coloured background shows the observational data in the corresponding cross-sections.

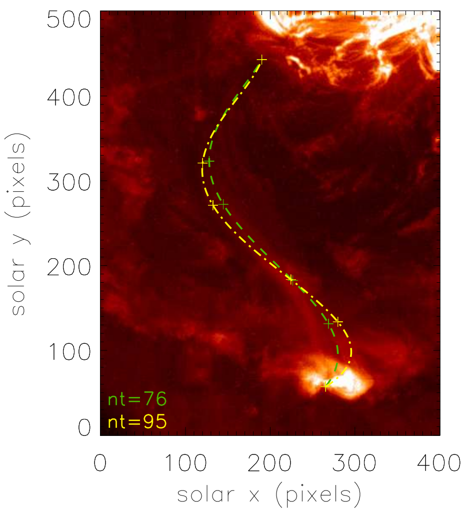

FIG. 5.— Polynomial fit to the loop displacements at two different times (dashed: nt=76; dot-dashed: nt=95).

which corresponds to the physical displacement of the entire loop structure as the flare 'blast wave' goes past. Subsequently, the central part settles into a smaller amplitude oscillation whereas both loop legs ('upper 1 & 2' and 'lower') show much larger, simultaneous displacements, characteristic of an even harmonic. The fact that this higher (even) harmonic is indeed spatially resolved by the observations is illustrated in Fig. 5, where two examples of the 'fitted' loop ($nt = 76$ and 95) are overplotted onto the snapshot $nt = 118$. Note that fits are not at the same time as the underlying TRACE data but were chosen because they clearly show the higher harmonic nature of the displacement.

To determine the dominant periods, we fit each of the measured displacements with a function of the following form,

$$fit = c_0 + c_1 t + \sum_{j=i}^{iii} A_j \sin\left(\frac{2\pi}{P_j} t + \phi_j\right) e^{-t/\tau_j} \, . \qquad (1)$$

The resulting fits are overplotted as dot-dashed lines in Fig. 2, with the fit parameters given in Table 1. In Fig. 3, we have plotted each of the oscillatory components (shifted by an arbitrary amount). The longest periods are of the order of 20 - 40 minutes (compared to 43 minutes for the total length of the time series) and they mainly occur in the later part of the dataset, where the loop strands are less easy to identify. Hence, we will focus on the two shorter periods, of the order of 577 - 672 sec and 250 - 346 sec. Comparing Figs. 2 and 3, it is clear that the loop displacement is dominated by the ∼630 sec period, which is out of phase in the upper and lower legs, and has a very small amplitude near the loop apex, characteristic of an even harmonic, standing mode.

The observed loop oscillation is most likely to be a standing, MHD kink wave and given the asymmetric nature of the loop displacements, it seems reasonable to assume that the ∼630 sec period is P_2, i.e. the period of the second harmonic. Measuring the distance between the two chosen loop footpoints (stars in Fig. 1), we find a loop 'base line' of ∼200 arcsec or ∼145 Mm. Assuming a semi-circular loop, this would give a loop length of L ∼228 Mm. As the loop is quite twisted, a semi-circle might not be the best approximation but it can probably be considered as a lower limit to the loop length. The wavelength of a second harmonic standing mode is equal to the loop length ($\lambda_2 = L$) and hence, we can estimate the phase speed as

$$v_{ph} = \frac{\lambda_2}{P_2} \approx 340 - 395 \text{ km/s} \, . \qquad (2)$$

In the thin tube approximation, there are two kink modes (see e.g. Roberts 1991), namely the slow and fast kink modes, which have phase speeds given by

$$c_T = \frac{c_s v_A}{\sqrt{c_s^2 + v_A^2}} \qquad \& \qquad c_k = v_A \sqrt{\frac{2}{1 + \rho_e/\rho_{loop}}} \, , \qquad (3)$$

respectively, where c_s and v_A are the sound and Alfvén speed and ρ_e and ρ_{loop} are the densities of the surrounding medium and the loop. In the solar corona, generally $v_A > c_s$ and hence $c_T < c_s$. For a temperature $T = 10^6 K$, the sounds speed is of the order of 150 km/s so we would expect $c_T < 150$ km/s. This is below the observed speed of about 365 km/s, leading us to conclude that the loop oscillations are likely to be fast MHD,

TABLE 1
OVERVIEW OF THE FIT DATA USED IN EQN. (1) FOR THE 4 CROSS SECTIONS.

	c_0	c_1	A_i	P_i	ϕ_i	τ_i	A_{ii}	P_{ii}	ϕ_{ii}	τ_{ii}	A_{iii}	P_{iii}	ϕ_{iii}	τ_{iii}
UPPER1	84.1	0.09	3.14	1806	1.41	6.6×10^9	-20.0	577	4.80	762	1.6	301	-0.6	3132
UPPER2	83.4	-0.06	5.07	1620	0.35	1.1×10^{10}	51.5	606	8.47	642	-2.08	295	1.66	2058
CENTRAL	23.6	-0.16	13.3	2484	1.92	1134	-0.43	672	2.26	-2544	13.9	346	5.29	771
LOWER	10.15	0.39	2.15	1038	9.54	1.1×10^{11}	-99.5	660	-5.85	521	13.3	250	-5.63	606

kink modes, in agreement with previous observations of transverse, flare induced loop oscillations (see e.g. Nakariakov et al 1999; Schrijver et al 2002; Aschwanden et al 2002). Our observed speed seems somewhat lower than previous estimates but due to the uncertainty in the loop length, the speed $v_{obs} \approx 365$ km/s is likely to only be a lower limit. For the upper and lower cross sections, the loop displacements are damped very rapidly (with damping times of the order of the periods), which is again in agreement with previously analysed examples.

The significance of the shorter periods (250 - 346 sec) is less clear. In the upper and central cross-sections, the values for P_{iii} are close to what would be expected for the fourth harmonic. Its presence at the 'central' location could be due to the fact that this cross section does not coincide exactly with the actual loop apex. However, for the lower cross section, the 250 sec period is closer to what would be expected for the fifth harmonic (P_5).

The combination of the observed displacements and the measured periods appears to be consistent with the presence of the second harmonic mode and possibly higher harmonics. However, the lack of the fundamental mode is hard to explain. One reason could be the fact that this is not one loop but two adjacent ones, with our 'apex' actually being an intermediate footpoint. However, this seems unlikely from a visual inspection and from the fact that the displacements in the upper and lower part of the loop are clearly out of phase, characteristic of an even higher harmonic. Additionally, it would be surprising to find such similar periods, excited by the same event, in neighbouring loops of different lengths. So this leaves us with two possibilities: either the fundamental mode is not excited (or only with a very small amplitude) or, alternatively, the fundamental mode is damped extremely quickly. One possible reason that the fundamental mode might not be excited, which is feasible, taking into account the relative positions of the flaring site and the loop system, is that the flare 'blast-wave' does not hit the loop centrally. Although one would expect the fundamental mode to be established eventually, the damping might be too strong to allow sufficient time for this to happen. Nakariakov et al (2004) demonstrate that the second standing acoustic harmonic is a natural response of a coronal loop to an impulsive energy deposition, whereas Brady & Arber (2005) show that damping through wave tunnelling leads to longer damping times for higher periods, i.e. higher harmonics would survive longer than the fundamental mode. However, both these studies focus on vertical loop displacements, rather than the transverse kink oscillations investigated here.

One factor which distinguishes this particular example from the other oscillating loops examined by Schrijver et al (2002) and Aschwanden et al (2002) is the fact that the loop appears much more twisted (i.e. have some kind of 'S-shape'), whereas most other examples seem closer to a semi-circular shape. However, determining whether higher harmonics would be preferentially excited in such 'S-shaped' loops would form a substantial study in itself and is beyond the scope of this present paper. Finally, we point out that the likely loop apex appears to be situated above a bright feature, leaving open the possibility that this underlying structure somehow affects the nature and amplitude of the loop oscillations. Additionally, it is feasible that a complex loop geometry, combined with unknown projection effects could give a fundamental mode the 'appearance' of a second harmonic.

In summary, we have found evidence of spatially resolved, higher harmonics in transverse, flare-induced loop oscillations, where the second harmonic (P_2) appears to dominate the oscillatory nature of the loop displacements. The apparent absence of the fundamental mode has strong implications for our modelling efforts. The mechanisms behind both the excitation and strong damping of these flare-induced loop oscillations are still much debated (see Nakariakov & Verwichte (2005) for a summary). A strong test for any suggested model would be to explain why in this particular case, the fundamental mode appears to be absent.

IDM acknowledges support of a Royal Society University Research Fellowship.

REFERENCES

Aschwanden, M.J., Fletcher, L., Schrijver, C.J., Alexander, D., 1999, ApJ 520, 880

Aschwanden, M.J., De Pontieu, B., Schrijver, C.J., Title, A., 2002, Sol. Phys. 206, 99

Brady, C.S., Arber, T.D., 2005, A&A 438, 733

De Moortel, I., 2005, Roy. Soc. Phil. Trans. A 363, 2743

McEwan, M.P., Donnelly, G.R., Díaz, A.J., Roberts, B., 2006, A&A 460, 893

Nakariakov, V.M., Ofman, L., DeLuca, E.E., Roberts, B., Davila, J.M., 1999, Science 285, 862

Nakariakov, V.M., Ofman, L., 2001, A&A 372, L53

Nakariakov, V.M., Tsiklauri, D., Kelly, A., Arber, T.D., Aschwanden, M.J., A&A 414, L25

Nakariakov, V. M., Verwichte, E., 2005, Living Reviews in Sol. Phys. 2, 3 (http://www.livingreviews.org/lrsp-2005-3)

Roberts, B., Edwin, P.M., Benz A.O. 1984 ApJ 279, 857

Roberts, B., 1991, in *Advances in Solar System MHD* (Eds. E.R. Priest & A.W. Hood), CUP, Cambridge

Schrijver, C.J., Aschwanden, M.J., Title, A., 2002, Sol. Phys. 206, 69

Verwichte, E., Nakariakov, V.M., Ofman, L, DeLuca, E.E., 2004, Sol. Phys. 223, 77